# The effects of feed force on rivet bucking bar vibrations

**Article** *in* International Journal of Industrial Ergonomics · September 2018

DOI: 10.1016/j.ergon.2018.05.011



**5 authors**, including:

Thomas W Mcdowell
Centers for Disease Control and Prevention
**81** PUBLICATIONS **1,038** CITATIONS
SEE PROFILE

Xueyan Sherry Xu
Centers for Disease Control and Prevention
**47** PUBLICATIONS **330** CITATIONS
SEE PROFILE

Chris M Warren
Centers for Disease Control and Prevention
**112** PUBLICATIONS **2,604** CITATIONS
SEE PROFILE

Daniel E Welcome
Centers for Disease Control and Prevention
**121** PUBLICATIONS **1,782** CITATIONS
SEE PROFILE

International Journal of Industrial Ergonomics 67 (2018) 145–158

Contents lists available at ScienceDirect

International Journal of Industrial Ergonomics

journal homepage: www.elsevier.com/locate/ergon

# The effects of feed force on rivet bucking bar vibrations

T.W. McDowell*, X.S. Xu, C. Warren, D.E. Welcome, R.G. Dong

*National Institute for Occupational Safety and Health (NIOSH), NIOSH Health Effects Lab, 1095 Willowdale Road, Morgantown, WV, 26505, USA*

ARTICLE INFO

*Keywords:*
Riveting
Hand-transmitted vibration
Risk assessment
Bucking bar
Feed force

ABSTRACT

Percussive riveting is the primary process for attaching the outer sheet metal "skins" of an aircraft to its airframe. Workers using manually-operated riveting tools (riveting hammers and rivet bucking bars) are exposed to significant levels of hand-transmitted vibration (HTV) and are at risk of developing components of hand-arm vibration syndrome (HAVS). To protect workers, employers can assess and select riveting tools that produce reduced HTV exposures. Researchers at the National Institute for Occupational Safety & Health (NIOSH) have developed a laboratory-based apparatus and methodology to evaluate the vibrations of rivet bucking bars. Using this simulated riveting approach, this study investigated the effects of feed force on the vibrations of several typical rivet bucking bars and that transmitted to the bucking bar operator's wrist. Five bucking bar models were assessed under three levels of feed force. The study results demonstrate that the feed force can be a major influencing factor on bucking bar vibrations. Similar feed force effects were observed at the bucking bar operator's wrist. This study also shows that different bucking bar designs will respond differently to variations in feed force. Some bucking bar designs may offer reduced vibration exposures to the bar operator's fingers while providing little attenuation of wrist acceleration. Knowledge of how rivet bucking bar models respond to riveting hammer vibrations can be important for making informed bucking bar selections. The study results indicate that, to help in the appropriate selection of bucking bars, candidate bar models should be evaluated at multiple feed force levels. The results also indicate that the bucking bar model, feed force level, or the bucking bar operator have no meaningful effects on the vibration excitation (riveting hammer), which further suggests that the test apparatus proposed by NIOSH researchers meets the basic requirements for a stable vibration source in laboratory-based bucking bar vibration assessments. This study provides relevant information that can be used to help develop a standardized laboratory-based bucking bar evaluation methodology and to help in the selection of appropriate bucking bars for various workplace riveting applications.

*Relevance to Industry:* Because the feed force level can affect HTV exposures to bucking bar operators, the feed force required for specific riveting operations should be an important consideration when selecting bucking bar models. This study provides useful information about bucking bar responses to riveting hammer vibrations; this knowledge can improve bucking bar selections.

## 1. Introduction

In the aerospace industry, percussive riveting is the primary process for attaching the outer sheet metal "skins" of an aircraft to its airframe during assembly and maintenance. Millions of rivets are required to attach the skin sections of a large continental aircraft; even a small, regional airplane or fighter aircraft requires hundreds of thousands of rivets (Campbell, 2006; Xi et al., 2013). Some aircraft riveting is accomplished using automated and semi-automated riveting machines, but due to the size and restricted maneuverability of these robotic devices, such automated processes are usually limited to large, flat substructures (Xi et al., 2013). For access to tighter spaces and for more complex sub-assembly shapes, a manual riveting process is often used. In the typical manual riveting process, metal rivets are individually-inserted into sheet metal with pre-drilled and countersunk holes. An operator uses a riveting hammer to sequentially set each rivet as it is driven against a metallic bucking bar held by a second tool operator positioned on the opposite side of the airframe (see Fig. 1). Even in this age of advanced robotics and innovative materials, this manual process still represents the principal method for fastening sheet metal skins to the frames of commercial and military aircraft throughout the world (Jorgensen and Viswanathan, 2005; Campbell, 2006; Cheraghi, 2008).

Workers using manually-operated riveting tools are exposed to significant levels of hand-transmitted vibration (HTV), and exposures to percussive HTV among riveters has become a major occupational health concern. Studies have shown that pneumatic percussive riveting

* Corresponding author. CDC/NIOSH/HELD, 1095 Willowdale Road, MS 2027, Morgantown, WV, 26505, USA.
*E-mail address:* TMcDowell@cdc.gov (T.W. McDowell).

https://doi.org/10.1016/j.ergon.2018.05.011
Received 9 November 2017; Received in revised form 20 March 2018; Accepted 17 May 2018

**Fig. 1.** Manual percussive riveting of aircraft sheet metal skins requires two riveting tool operators; one worker operates the riveting hammer (left) on the exterior surface of the assembly, while a second worker operates the bucking bar (right) on the interior of the airframe. The riveting hammer delivers a rapid series of impacts while the bucking bar supplies the opposing force. The metal rivet is mechanically deformed and work-hardened between the two riveting tools to securely fasten the sheet metal to the airframe.

hammers can produce high vibration magnitudes (Dandanell and Engstrom, 1986; Burdorf and Monster, 1991; McDowell et al., 2012). This percussive vibration can be effectively transmitted to the hands and fingers of the riveting hammer and bucking bar operators (Kattel and Fernandez, 1999). Riveting-induced HTV has been associated with the development of components of hand-arm vibration syndrome (HAVS) such as vibration white finger (VWF) (Yu et al., 1986; Burdorf and Monster, 1991). It has been reported that in some occupational environments, perhaps more than 50% of riveting tool operators could exhibit symptoms of HAVS within the first decade of their careers (Engström and Dandanell, 1986; Burdorf and Monster, 1991). Combinations of intensive HTV exposures, forceful exertions, repetitive actions, and awkward hand and finger postures may leave bucking bar operators especially vulnerable (McKenna et al., 1993; Fredericks and Fernandez, 1999). These ergonomic factors could also be connected with increased incidences of carpal tunnel syndrome and other hand and wrist musculoskeletal disorders among sheet metal workers (Burdorf and Monster, 1991; NIOSH, 1997). The underlying biomechanics involved in the development of HAVS are largely unknown, but several studies have implicated percussive HTV in the etiology of the syndrome. In a study using a rat-tail model, Govinda Raju et al. (2011) concluded that percussive vibrations designed to simulate rivet bucking bar HTV exposure may cause severe nerve damage. Krajnak et al. (2013) also reported that impact vibration may adversely affect peripheral nerves. Percussive HTV has also been associated with damage to joint cartilage (Gemne and Saraste, 1987). Exposures to rivet bucking bar vibrations have also been linked to acute vascular effects in workers (McKenna et al., 1993). Further, impulse vibrations have been shown to cause damage to red blood cells in vitro (Ando et al., 2005).

Because of the strong association between percussive HTV exposures and the above-mentioned health concerns, it has become accepted practice at many workplaces to develop HTV exposure control strategies in efforts to help minimize the potential for harm. In many parts of the world, employers are required by law to implement HTV exposure control programs (EU Directive, 2002). Guidelines and/or requirements for HTV control programs are found in national and international standards for assessing and controlling occupational HTV exposures; most of these HTV exposure standards incorporate aspects of the International Organization for Standardization (ISO) standards for measuring and assessing HTV exposures (ISO 5349-1, 2001a; ISO 5349-2, 2001b). In the European Union, EU Directive 2002/44/EC on human vibration exposure requires that HTV exposure assessments be conducted in accordance with these ISO standards (EU Directive, 2002). The EU Directive also specifies a daily Exposure Action Value (EAV) and a daily Exposure Limit Value (ELV). These values represent the upper boundaries on the daily HTV exposure values normalized to an 8-h work shift. In the U.S., provisions of the EU Directive including the EAV and ELV are repeated in the U.S. HTV exposure standard (ANSI S2.70, 2006).

Responsibility for HTV exposure control typically falls on the employer, and the above-mentioned national and international standards form the foundation for most employer's HTV control programs. The standards instruct employers to first focus on reducing HTV at the source (EU Directive, 2002; ANSI S2.70, 2006), so it is typical for employers to implement practices for identifying and selecting powered hand tools that generate reduced HTV exposures. The SAE International Aerospace Standard AS6228 (SAE, 2014) provides technical guidance for power hand tool selection which includes evaluations of life-cycle cost, productivity, and safety/health factors, including HTV exposures. In order to compare tool models based on their vibration emissions, the tools should be assessed while they are challenged under comparable operating conditions. Ideally, the tools should be assessed while being operated during the actual work tasks for which they are intended to be used. However, it is usually very difficult to maintain consistent trial-to-trial tool loading conditions in workplace environments. Such systematic workplace tool vibration assessments may also be time-consuming and expensive; obtaining statistically-reliable tool model comparisons usually requires many tool operators due to potentially-large intra-operator and inter-operator variations. The costs increase substantially when multiple tool models are involved in the tool assessments. Alternatively, tool vibration comparisons can be conducted in a laboratory using a simulated workstation whereby different tools can be tested under comparable tool loading conditions. While not suitable for assessing workplace vibration exposures, laboratory testing can be used for initial screenings to predict which tool models might be expected to produce lower vibration exposures in the workplace. To standardize such tool assessments and to make inter-laboratory results directly comparable, the ISO has developed the ISO 28927 series of laboratory-based tool vibration testing standards. These standards are intended to be used for comparing tools according to their tool handle vibrations. These standards prescribe the postures and loading conditions under which the tools will be evaluated. For example, Part 10 of this series (ISO 28927-10, 2011) pertains specifically to chipping hammers and riveting hammers. Researchers at the U.S. National Institute for Occupational Safety & Health (NIOSH) found that ISO method is acceptable for identifying riveting hammers that could be expected to exhibit lower vibrations in workplace environments (McDowell et al., 2012). Unfortunately, there is no standardized method for comparing rivet bucking bars in terms of their vibration exposures. To that end, a recent NIOSH study included the development of a laboratory-based method for evaluating bucking bar vibrations (McDowell et al., 2015). That study found that the NIOSH test method shows promise for identifying rivet bucking bar designs that may reduce workplace HTV exposures to sheet metal workers, but the bucking bar test method is in need of some refinements.

One refinement to the bucking bar test being explored requires an examination of the effect of feed force on the measured vibration. The level of hand forces applied to a vibrating tool by the tool operator has been shown to affect the HTV exposure, so the control of feed force has traditionally been included in standardized laboratory-based tool vibration assessments (e.g., ISO 8662-2, 1992; ISO 8662-7, 1997). Many studies have indicated that increasing the hand forces applied to a tool

handle leads to increased system stiffness, and in turn increased vibration transmission and energy absorption (Burström and Lundström, 1994; Marcotte et al., 2005; Besa et al., 2007). Dong et al. (2005) found that the push force, or feed force, has a more pronounced effect on the hand-arm system biodynamic response than does grip force. Feed force has also been shown to be a significant factor in measurements of tool vibrations during standardized vibration assessments of percussive tools (Dong et al., 2004).

The results of these previous studies indicate that feed force may be an important consideration when evaluating the HTV of rivet bucking bars and also when making informed selections of bucking bar models. However, the feed force effect on bucking bar vibration has not been reported. Therefore, the primary objective of this study is to examine the effect of feed force on the vibration measured at the bucking bar as well as at the wrist of the bucking bar operator. Traditional cold-rolled steel bucking bars were used in the evaluation along with reduced-vibration bucking bars featuring tungsten alloys or spring-damper shock-absorbing systems. This information can be used to help refine the laboratory-based bucking bar vibration assessment method developed in our earlier study (McDowell et al., 2015). This information should also be useful for making appropriate bucking bar selections for different riveting operations.

## 2. Methods

### 2.1. Bucking bar operators

Eight healthy volunteer test subjects (seven male, one female) were recruited locally to operate the bucking bars in this study. Anthropometry data are presented in Table 1. All eight bucking bar operators were right-handed. These recruits had no experience with sheet metal riveting tools. With informed consent, the recruited tool operators followed a protocol that was reviewed and approved by the NIOSH Human Subjects Review Board. During the experiments, the bucking bar operators wore casual clothing, regular work gloves, safety glasses, and hearing protection.

### 2.2. NIOSH lab-based test apparatus for assessing bucking bar vibration

The experiments were conducted using an updated version of the laboratory-based apparatus and methodology for simulating a riveting task and evaluating rivet bucking bar vibrations developed in a recent NIOSH study (McDowell et al., 2015). The NIOSH approach (see Fig. 2) is similar to the lab evaluations presented in the ISO 28927 series for hand-held non-electric tools where sample tools within a tool group are operated by human test subjects against a specified, consistent load while the vibration emissions are measured near where the vibration enters the tool operator's hand. The NIOSH-designed bucking bar HTV assessment method employs several features and techniques presented in those existing ISO standardized methodologies (e.g., ISO 28927-10, 2011). Similar to the ISO standards, the NIOSH apparatus and procedure are designed to deliver consistent forces and excitation to selected bucking bars while the vibration transmitted to the hand-tool interface is measured. To provide the vibration stimulus, an Ingersoll-Rand Model AVC 13 size 4X riveting hammer is securely-mounted on one side of an energy absorber. The energy absorber is a modified version of the one that was developed by engineers at Atlas Copco Tools AB for their bucking bar test stand and procedure (Treskog, 1994). Basically, the energy absorber is a steel cylinder filled with hardened steel balls and is very similar to that described in the standardized method for evaluating riveting hammers and related percussive tools (ISO 28927-10, 2011). The energy absorber assembly (Fig. 2(D)) is mounted horizontally on a rigid, heavy steel fixture that is bolted on top of a large reinforced-concrete base. An anvil-shaped riveting bit is inserted into the riveting hammer, and the anvil-shaped end rests against the column of hardened steel balls inside the cylinder. A second anvil-shaped bit (Fig. 2(E)) is inserted into the opposite end of the energy absorber to mirror the riveting hammer bit; this second rod serves as the simulated rivet. As the riveting hammer operates, energy is transferred from the riveting bit to the column of steel balls, and then to the simulated rivet. The energy absorber dissipates some of the energy which enables stable and reproducible inputs to the simulated rivet.

During the experiments, the bucking bar operator grasps a bucking bar with his/her dominant hand while using the non-dominant hand for additional support and control (see Fig. 2). The operator presses the flat surface of the bucking bar against the vibrating simulated rivet. To measure the applied feed force, the operator stands on a force plate (Fig. 2(A)) mounted on a wooden platform; the platform height is adjusted as necessary so that the operator can comfortably perform the simulated riveting task. The applied feed force is displayed as a strip chart on a computer monitor placed in front of the operator (Fig. 2(B)). During the simulated riveting trials, tri-axial acceleration data are collected at the riveting hammer, at the surface of the bucking bar, and at the wrist of the operator (dominant side).

**Table 1**
Anthropometry of the eight bucking bar operators. Hand length is from the tip of the middle finger to the crease at the wrist. Width is at the distal end of the metacarpals. Volume is the amount of water displaced by the right hand submerged to the crease at the wrist.

| Operator | Sex | Stature (m) | Weight (kg) | Hand Length (mm) | Hand Width (mm) | Hand Volume (ml) |
|---|---|---|---|---|---|---|
| A | M | 1.85 | 90.9 | 201 | 93 | 455 |
| B | F | 1.60 | 104.7 | 189 | 81 | 330 |
| C | M | 1.93 | 87.3 | 209 | 91 | 455 |
| D | M | 1.82 | 128.3 | 197 | 83 | 470 |
| E | M | 1.83 | 90.4 | 206 | 83 | 435 |
| F | M | 1.73 | 84.3 | 193 | 78 | 418 |
| G | M | 1.75 | 77.6 | 182 | 78 | 357 |
| H | M | 1.76 | 76.4 | 178 | 86 | 398 |
| Mean | | 1.78 | 92.5 | 194 | 84 | 415 |
| SD | | 0.10 | 17.0 | 11 | 6 | 50 |

### 2.3. Rivet bucking bars

Five rivet bucking bar models were used in this study. Fig. 3 shows a sample of each bucking bar model, while Table 2 provides descriptions of each model. One model (bar A) is a traditional cold-rolled steel bar (ATI Tools/Snap-on Specialty Tools, City of Industry, CA, USA), one model (bar B) is a heavier tungsten alloy bar with the same shape and size as the steel bar (Honsa Ergonomic Technologies, Milan, IL, USA), and three models (bars C, D, and E) feature spring-damper configurations. Bars C and D are Atlas Copco models (Atlas Copco Tools, Auburn Hills, MI, USA), while bar E is manufactured by U.S. Industrial Tool Company (Gardena, CA, USA). Two samples of each model were used in the study.

### 2.4. Test matrix/procedure

Three feed force levels were evaluated in the study: 40 ± 10 N, 65 ± 10 N, and 90 ± 10 N. During a test session, the bucking bar operator completed three trials with each bucking bar/force level combination. Thus, the test session matrix consisted of 90 trials per operator (5 bucking bar models × 2 samples per model × 3 force levels × 3 trials per combination). Each operator's test session was divided into halves; one sample of each bar model was used in the first half, and the second sample of each model was used in the second half. The pre-determined test matrix order was independently randomized for each bucking bar operator; the order of the bar models was randomized within each half-session, while the force level order was randomized for each bucking bar. A complete test session lasted about

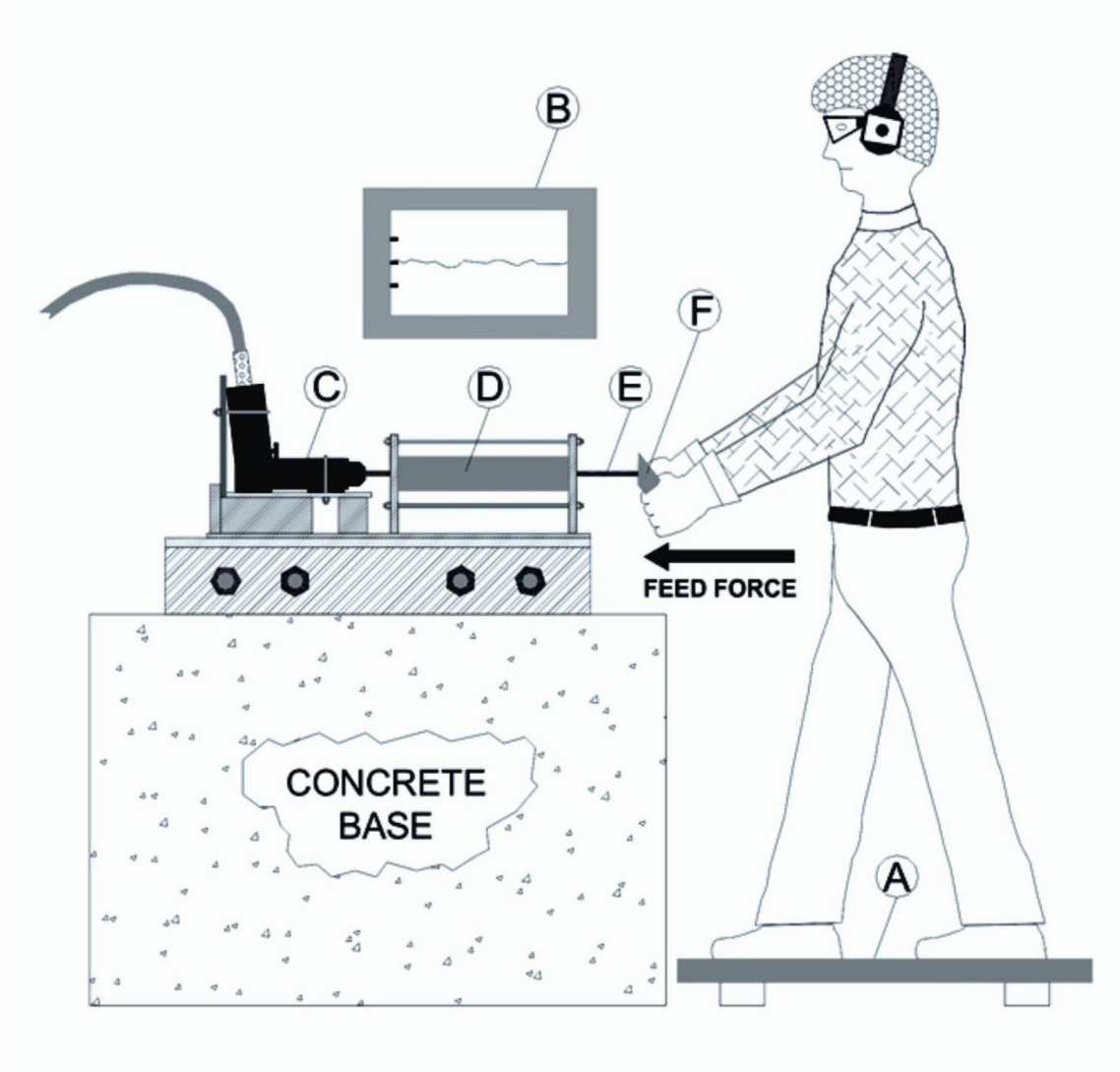


**Fig. 2.** Experimental setup and posture of the bucking bar operator pressing the bar against the simulated rivet. (A) Force plate measures the ground reaction force (feed force); (B) Computer monitor displays the applied feed force as a strip chart allowing the bucking bar operator to maintain the target force within the specified range; (C) Remote-controlled pneumatic riveting hammer programmed to deliver consistent vibration stimuli; (D) Energy absorber dampens the vibration input to the simulated rivet; (E) Simulated rivet; (F) Bucking bar is pressed against the simulated rivet. Tri-axial acceleration data was simultaneously collected at the riveting hammer, the bucking bar, and at the right wrist of the bucking bar operator.

2.5 h including time for reading/signing the consent form, anthropometry data collection, and practice trials.

During the test, the on/off operation of the riveting hammer mounted on the test apparatus was remote-controlled via a control station manned by the NIOSH investigator. The control station features a repeat-cycle timer that was programmed to automatically cycle power to the tool air supply solenoid valve which cycled the riveting hammer on and off. (A schematic and other details of this control system can be found in the online supplemental material published with the report of our earlier rivet bucking bar study (https://doi.org/10.1093/annhyg/meu091) (McDowell et al., 2015). To mimic typical aircraft sheet metal riveting operations, the simulated riveting cycle consists of 2 s on time and 3 s off time per rivet. A single trial in the NIOSH lab test simulates the setting of 5 rivets in 30 s.

Prior to a set of trials, a NIOSH engineer prepared the designated bucking bar for operation and data collection. The engineer handed the prepared bucking bar to the bucking bar operator who assumed the prescribed posture to complete the first trial. Each bucking bar operator underwent a familiarization period with the bucking bar operation, the simulated riveting cycles/vibration generated by the test apparatus, and with the feed force monitoring system. If necessary, the platform height was adjusted to ensure comfort and proper work posture. The operator performed a number of practice trials. Once comfortable with the procedure, the operator began the series of data collection trials.

To begin a trial, the operator was instructed to press the flat surface of the bucking bar against the simulated rivet with the specified feed force. Once the feed force was observed to be stable, the NIOSH investigator initiated a 30-s vibration exposure/data collection trial by pressing the start button on the remote-control station. The bucking bar operator was instructed to try to maintain a steady feed force while the simulated rivet cycled through the 5-rivet sequence. At the end of the 30-s trial, the operator rested for at least 1 min. The bucking bar operator completed three consecutive trials with the prescribed bucking bar/feed force level. At the completion of three trials, the coefficient of variation (CV) of the ISO frequency-weighted total value ($a_{hv}$) was immediately calculated for those trials. As is specified in the ISO 28927 series of standards, trials were repeated if the CV was found to be 0.15 or greater. Once three satisfactory trials were completed, the feed force monitoring system was reset to the next prescribed feed force level, and the process was repeated for that feed force level. Once the operator

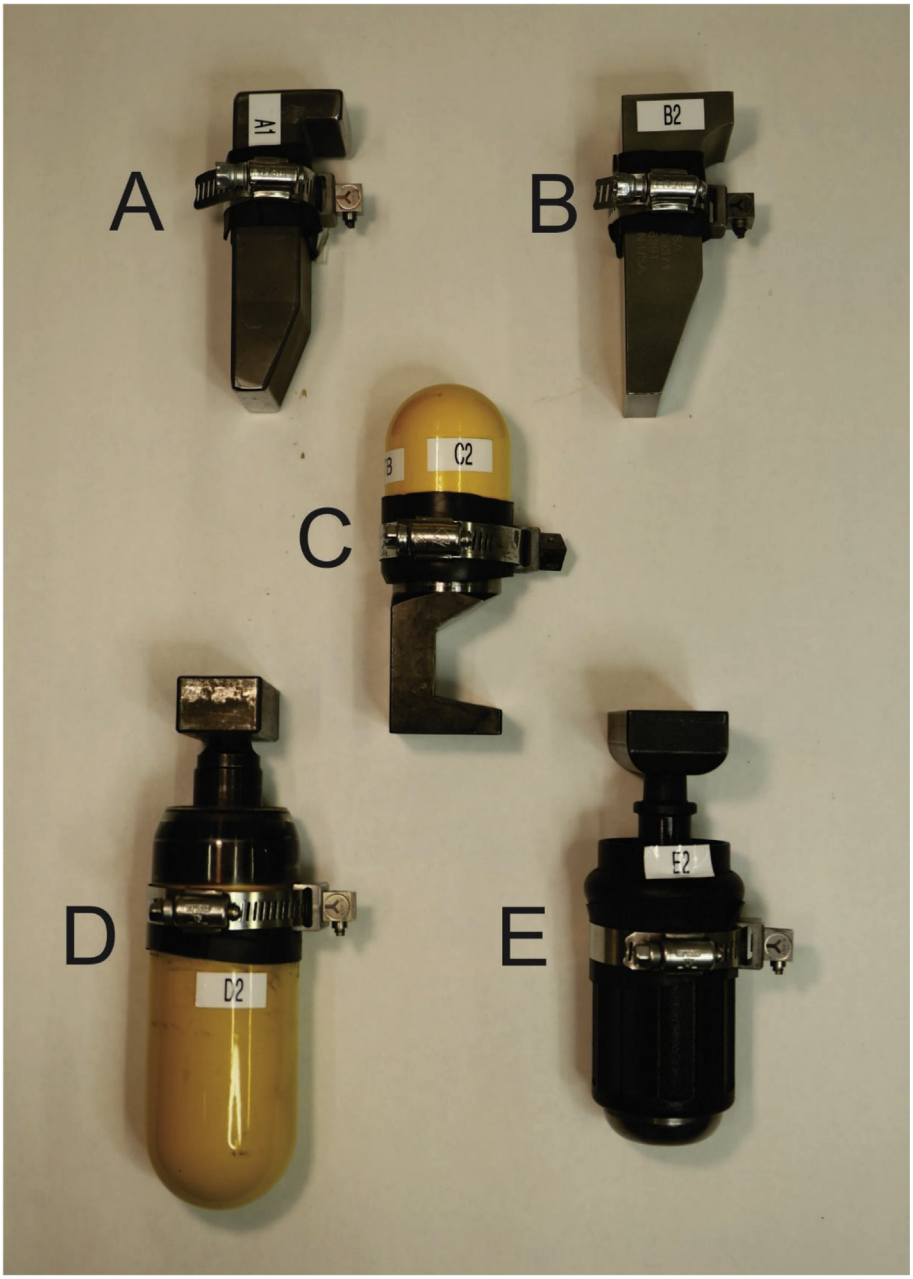


**Fig. 3.** The five rivet bucking bar models used in the study with their accelerometers mounted with hose clamps. Two samples of each model were used by each operator at each of the three feed force levels. Descriptions of each bucking bar model (A–E) are provided in Table 2.

**Table 2**
Descriptions of the five rivet bucking bar models. Two samples of each bar model were used in the study.

| Bar ID | Manufacturer | Model | Weight (kg) | Type |
|---|---|---|---|---|
| A | ATI Tools | AT639 | 0.87 | cold rolled steel |
| B | Honsa | TBBT639T | 2.10 | tungsten alloy |
| C | Atlas Copco | RBB 04SP-06 | 1.12 | recoilless dampener |
| D | Atlas Copco | RBB 10SP | 1.47 | recoilless dampener |
| E | U.S. Industrial Tool | TP111R (handle) TP1510A (dolly) | 1.09 | recoilless dampener |

had completed three trials with a particular bucking bar at each feed force level, the NIOSH engineer prepared the next bar, and the process was repeated.

### 2.5. Accelerometers and vibration data collection systems

The bucking bar acceleration data was collected at the surface of the bucking bar in close proximity to where the vibration enters the operator's hand (see Figs. 3 and 4). The riveting hammer accelerometer was clamped to the body of the riveting hammer near the bit chuck (see Fig. 4). All bucking bar and riveting hammer vibration measurements were collected via PCB Model 356B11 piezoelectric tri-axial accelerometers (PCB Piezotronics, Depew, New York). As shown in Fig. 4, the accelerometers were installed on mounting blocks and secured to the bucking bars and riveting hammer using hose clamps. Once each accelerometer was installed, the accelerometers and mounting

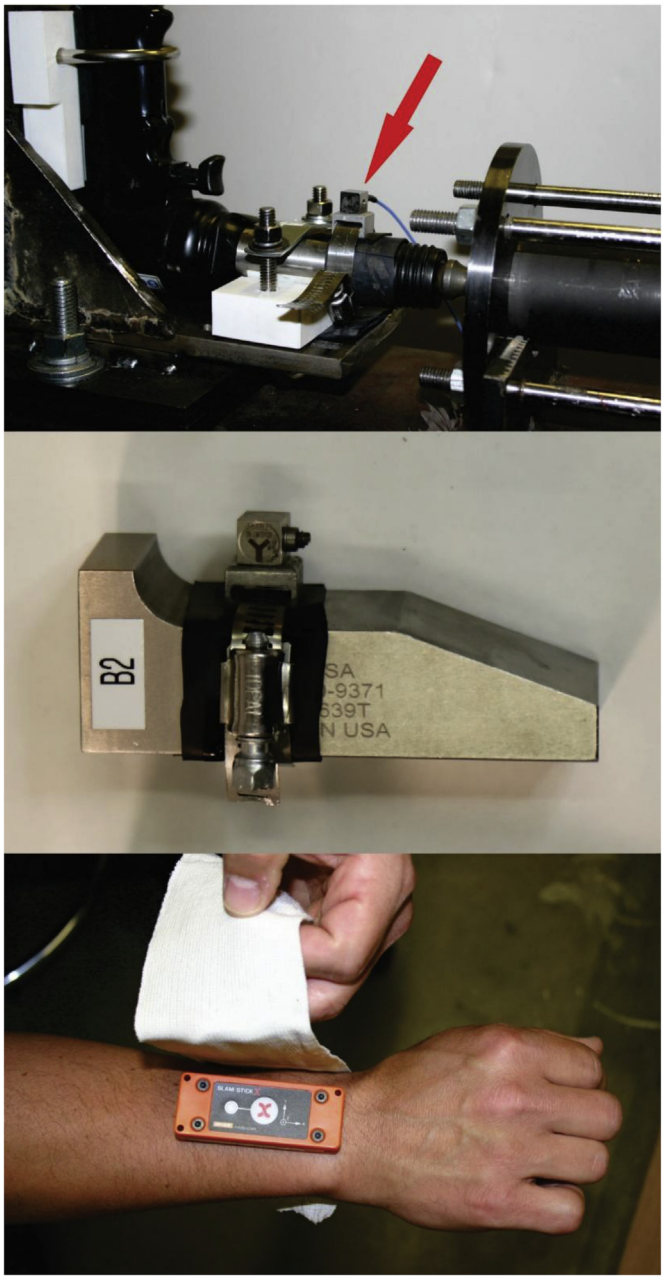


**Fig. 4.** PCB Model 356B11 piezoelectric tri-axial accelerometers (PCB Piezotronics, Depew, New York) were attached to the riveting hammer (vibration source) and each bucking bar using hose clamps. Synthetic rubber was used as a mechanical filter to prevent DC shifts in the acceleration signals. Tri-axial acceleration data at the right wrist of each bucking bar operator was collected via a Slam Stick X accelerometer/data logger (Midé Technology, Boston). The Slam Stick X was attached to the wrist using an elastic cloth bandage wrap.

assemblies were wrapped with electrical tape to prevent hand contact with any sharp edges. The measurement of vibration of percussive tools often yields significant direct current (DC) shifts in the piezoelectric accelerometer output (Griffin, 1990). These DC shifts are a source of measurement error and should be mitigated. Consequently, a layer of synthetic rubber was used as a mechanical filter to minimize or eliminate the DC shift. This synthetic rubber layering technique has been proven to be successful in several earlier experiments involving impact tools (Dong et al., 2004; McDowell et al., 2009, 2012). The effectiveness of this accelerometer installation technique was verified in the previous NIOSH bucking bar study by conducting a series of simultaneous vibration data collection trials with each bucking bar using a laser vibrometer along with the installed accelerometers (McDowell et al., 2015). (Measurements from a laser vibrometer are immune to the DC shifting problem.)

Bucking bar and riveting hammer tri-axial vibration data were collected simultaneously at a sampling frequency of 4096 Hz via a portable six-channel B&K PULSE system (Brüel & Kjær, Input/Output Module Type 3032A). Simultaneously with the bucking bar and riveting hammer acceleration, tri-axial acceleration data at the right wrist of each bucking bar operator was collected at a sampling frequency of 5000 Hz via a Slam Stick X accelerometer/data logger (Midé Technology, Boston, MA, USA). The Slam Stick X was secured to the wrist using an elastic cloth bandage wrap (see Fig. 4). The time history data from the Slam Stick X was downloaded to a PC; this data was processed using algorithms developed in-house using MATLAB® (MathWorks, Natick, MA, USA) and Microsoft Excel software.

### 2.6. Data processing and statistics

The acceleration data were expressed as the root-mean-square (r.m.s.) values of the accelerations in the one-third octave frequency bands, with center frequencies from 6.3 to 1250 Hz. Both time-history data and frequency spectrum were recorded for all three data collection locations. The vector sum, or 'total' values of the unweighted r.m.s. accelerations were computed using the following formula:

$$a_h = \sqrt{a_{hx}^2 + a_{hy}^2 + a_{hz}^2} \quad (1)$$

where $a_h$ is the unweighted root-sum-of-squares total value, and $a_{hx}$, $a_{hy}$, and $a_{hz}$, are the unweighted r.m.s. acceleration values for the x-, y-, and z-axis, respectively.

To determine the ISO frequency-weighted acceleration values for each axis, an Excel spreadsheet was used to apply the frequency-weighting factors defined in ISO 5349-1 (2001a):

$$a_{hw} = \sqrt{\sum_{j=1}^{24} (K_j a_{h,j})^2} \quad (2)$$

where $a_{hw}$ is the single-axis frequency-weighted r.m.s. acceleration, $K_j$ is the weighting factor for the $j$th one-third octave band as provided in Table 2 of the standard, and $a_{h,j}$ is the acceleration measured in the $j$th one-third octave band. In this process, the 24 one-third octave frequency band r.m.s. accelerations are multiplied by their respective weighting factors, and the resultant weighted r.m.s. accelerations are determined for each axis.

Then, as was done with the unweighted acceleration, the total ISO frequency-weighted values are computed using

$$a_{hv} = \sqrt{a_{hwx}^2 + a_{hwy}^2 + a_{hwz}^2} \quad (3)$$

where $a_{hv}$ is the ISO frequency-weighted root-sum-of-squares total value, and $a_{hwx}$, $a_{hwy}$, and $a_{hwz}$ are the ISO frequency-weighted r.m.s. acceleration values for the x-, y-, and z-axis, respectively.

General Linear Models of analysis of variance (ANOVA) for acceleration were conducted to evaluate the influence of feed force (three levels), bucking bar model (five levels), and the interaction of those two fixed factors on bucking bar, riveting hammer, and wrist acceleration. Separate analyses were completed for frequency-weighted and unweighted acceleration. Tukey Honestly Significant Difference (HSD) post hoc pairwise comparisons were also performed. All statistical analyses were performed using SPSS statistical software (IBM SPSS Statistics, version 24.0). Analysis results were considered significant at the $p < 0.05$ level.

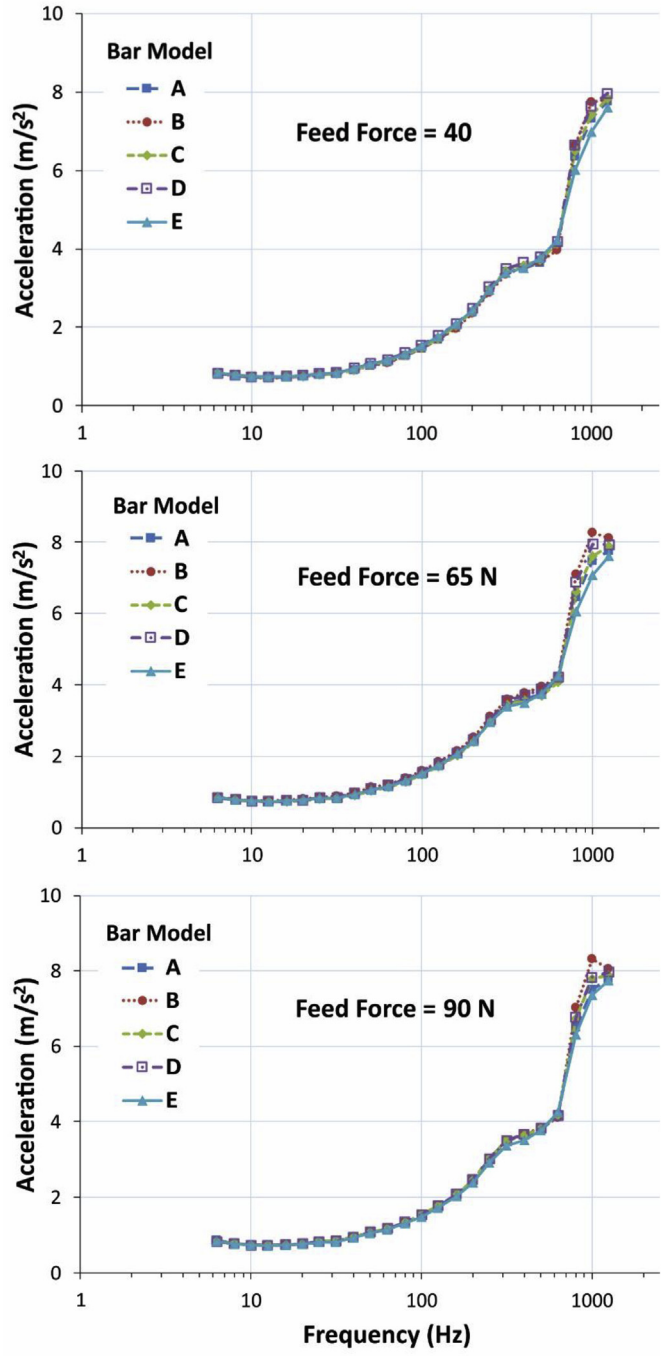


**Fig. 5.** The average one-third octave band vibration frequency spectra measured at the riveting hammer (vibration source) for the five bucking bar models (A–E) for each of the three feed force levels.

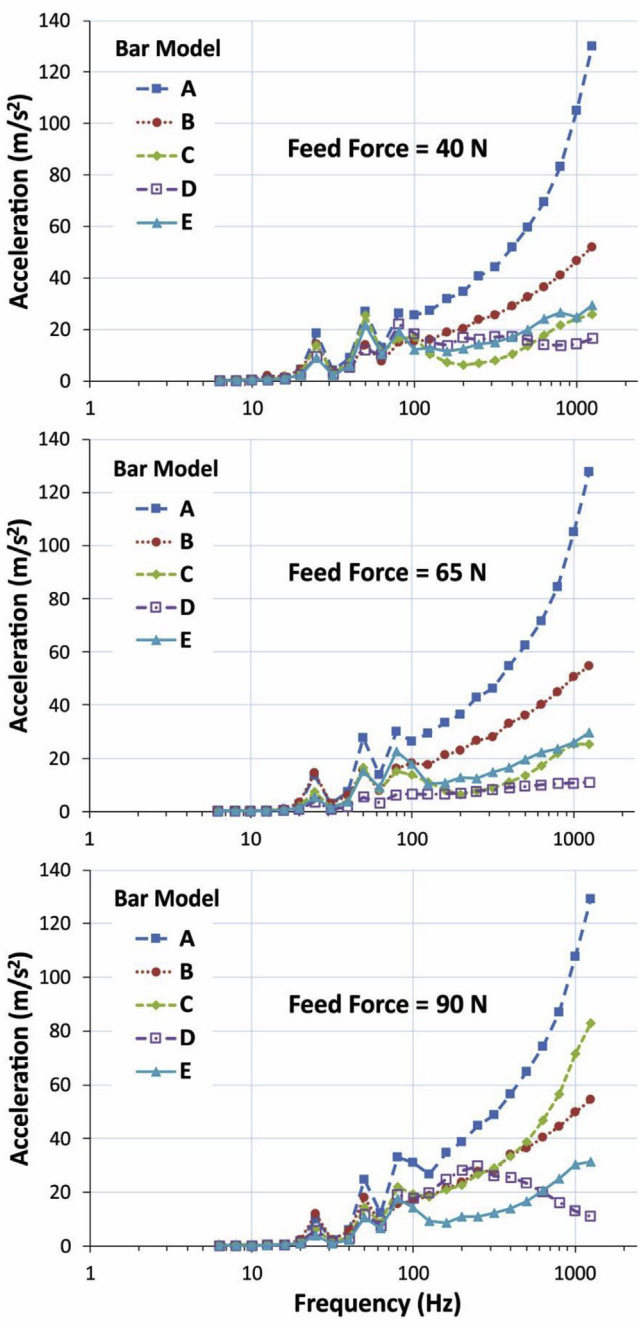


**Fig. 6.** The average one-third octave band vibration frequency spectra measured at the bucking bar for the five bucking bar models (A–E) for each of the three feed force levels.

## 3. Results

### 3.1. Vibration at the riveting hammer (vibration source)

The average vibration spectra measured at the housing of the riveting hammer near the bit chuck are pictured in Fig. 5. There are no noticeable differences among the bar models or feed force levels. The frequency-weighted and unweighted accelerations of the rivet hammer remained relatively steady throughout all the combinations of the bucking bar, feed force, and tool operator. The ANOVA and post hoc Tukey tests for frequency-weighted acceleration revealed no significant feed force effect or bar model effect. The weighted acceleration means for the bucking bar models ranged from 1.9 to 2.0 m/s$^2$. The means for the three force levels were all equal at 1.9 m/s$^2$. The unweighted riveting hammer acceleration was also fairly stable; while the ANOVA revealed a significant feed force effect ($F_{2,705} = 3.8$; $p < 0.05$), the force level means ranged only from 15.7 m/s$^2$ for the 40 N force level to 16.1 m/s$^2$ for the 90 N force level. The bucking bar model effect was also statistically-significant ($F_{2,705} = 10.3$; $p < 0.01$), but the bar model means also fell within a small range (15.4 m/s$^2$ for bar model E to 16.4 m/s$^2$ for bar model B).

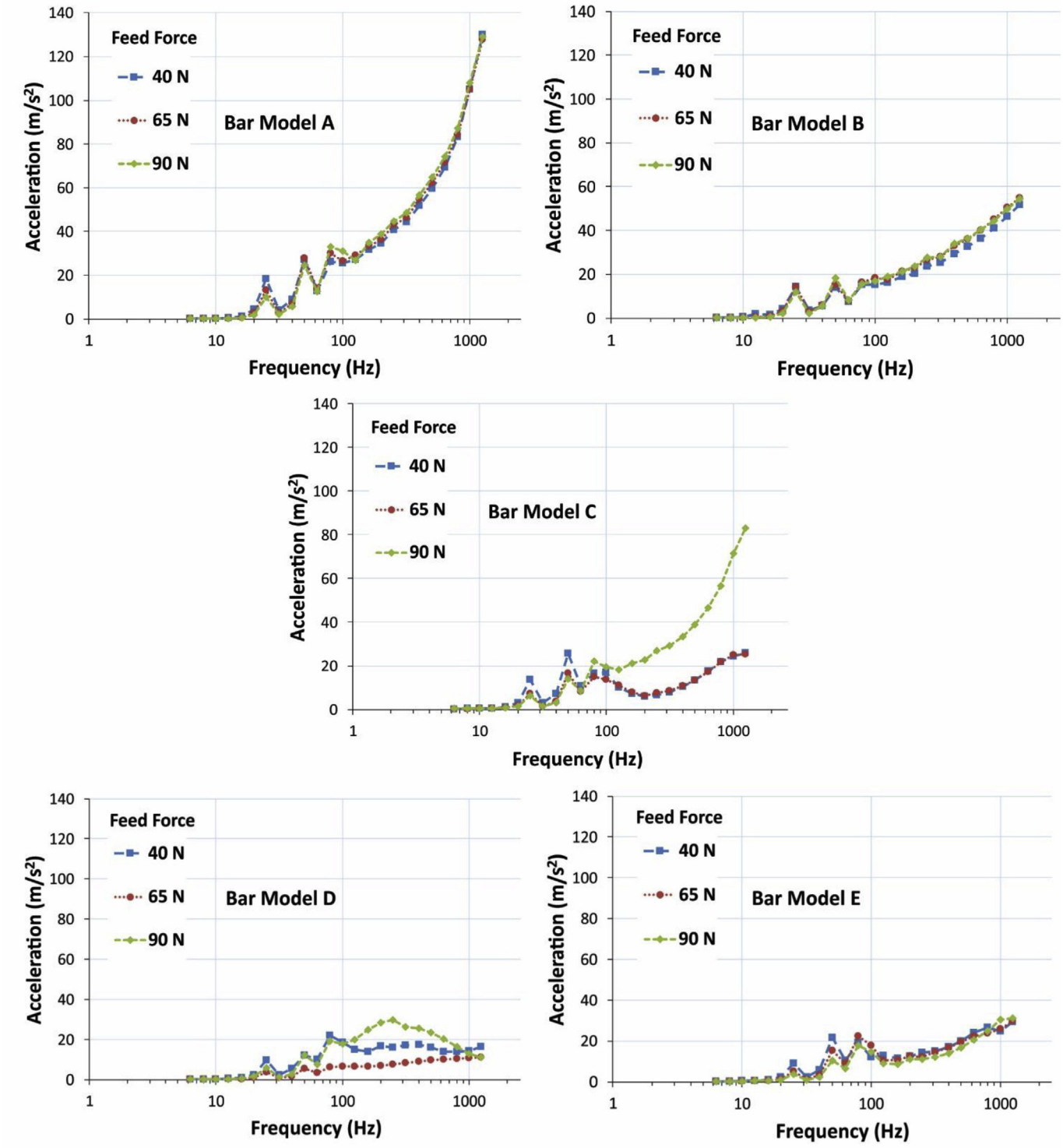


**Fig. 7.** The effect of feed force on the average one-third octave band vibration frequency spectra measured at the bar for each bucking bar model.

### 3.2. Bucking bar vibration

To compare bucking bar models, Fig. 6 shows the average one-third octave band vibration frequency spectra measured at the bucking bar for each bar model at each feed force level. Fig. 7 illustrates the effect of feed force on the vibration spectra for the individual bucking bar models. As shown, for all bar models and feed force levels, the first major peaks occur at 25 Hz, and the second major peaks occur at 50 Hz. While the spectra for the solid metal bars (bar models A and B) and the spring-damper bar model E are relatively similar at all feed force levels, the spectra for the spring-damper Atlas Copco bucking bar models C and D show considerable differences in the middle and higher frequency ranges across the three force levels. For example, bar C exhibits much higher acceleration at the higher frequencies at the 90 N force level, and bar D exhibits a substantial peak at 250 Hz for the 90 N force level that does not exist at the two lower force levels.

Fig. 8 shows the frequency-weighted and unweighted acceleration averages calculated from the vibration spectra measured at the bucking

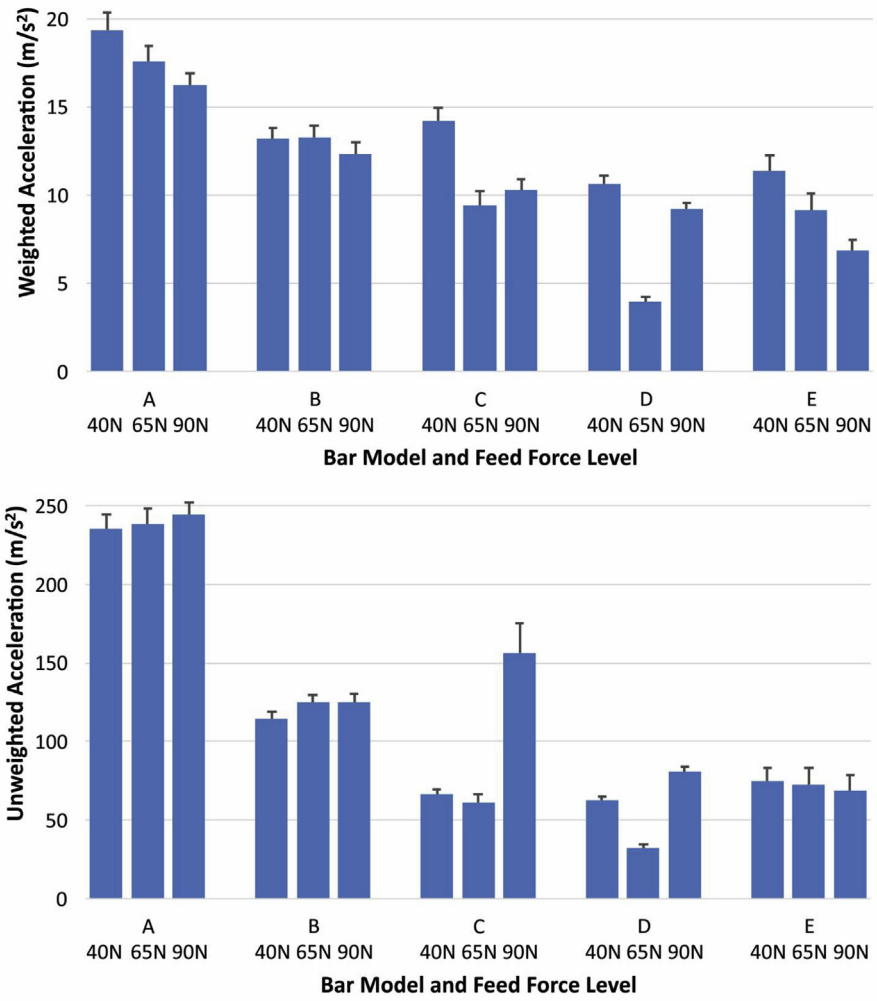


**Fig. 8.** The means for frequency-weighted acceleration (top graph) and unweighted acceleration (bottom graph) measured at the bucking bar for each bucking bar model (A–E) and feed force level. Error bars = standard error of the mean (SEM).

bar for each bucking bar model for each of the three levels of feed force. As shown in the figure, the traditional cold-rolled steel bar (bar A) exhibited the highest averages for both weighted and unweighted acceleration at all three force levels. In terms of frequency-weighted acceleration, the solid-metal bars (bars A and B) tended to have decreased acceleration as the feed force increased. The opposite trend emerged in terms of unweighted acceleration for these two bars. The two spring-damper Atlas Copco bars (bars C and D) exhibited their lowest weighted and unweighted acceleration averages at the middle feed force level (65 N). As can also be seen in the figure, these two bars were much more sensitive to the feed force effect as compared to the solid-metal bars and the spring-damper U.S. Industrial Tool bar (bar E). Bar E showed gradually decreased acceleration with the increase in feed force in terms of both weighted and unweighted acceleration.

The ANOVA for frequency-weighted acceleration measured at the bucking bar indicated that force level ($F_{2,705} = 146.2$; $p < 0.001$), bar model ($F_{4,705} = 442.5$; $p < 0.001$), and the force level by bar model interaction ($F_{8,705} = 31.3$; $p < 0.001$) were all significant factors. The ANOVA results were the same for unweighted bucking bar acceleration; force level ($F_{2,705} = 89.3$; $p < 0.001$), bar model ($F_{4,705} = 1090.3$; $p < 0.001$), and the force level by bar model interaction ($F_{8,705} = 41.5$; $p < 0.001$) were all significant factors. The middle feed force level (65 N) produced the lowest mean in terms of both frequency-weighted and unweighted acceleration. Post hoc Tukey tests showed that for frequency-weighted acceleration, the acceleration mean for the 40 N feed force trials was significantly higher than those for the two higher feed force targets (65 N and 90 N) ($p < 0.05$); the means for the 65 N and 90 N trials were not statistically different ($p > 0.05$). For unweighted acceleration, all means were significantly different from one another; the lowest feed force (40 N) produced the highest acceleration followed by the highest feed force (90 N) and the middle feed force (65 N). Tukey test results for bar model acceleration means were identical for frequency-weighted and unweighted acceleration; all bar models were significantly different from one another ($p < 0.05$). Ranking the bar models from highest to lowest acceleration was as follows: A, B, C, E, D.

### 3.3. Vibration at the wrist of the bucking bar operator

The average vibration spectra measured at the wrist for each bucking bar model at each feed force level are pictured in Fig. 9. Fig. 10 illustrates the effect of feed force on the wrist vibration spectra for the individual bucking bar models. Like the spectra measured on the bucking bars (Figs. 6 and 7), the first major peaks occur at 25 Hz, and the second major peaks occur at 50 Hz. Unlike the spectra measured at the bucking bars, wrist acceleration frequencies above 250 Hz are negligible for all bar models and feed force levels.

Fig. 11 shows the frequency-weighted and unweighted acceleration averages measured at the wrist for each bucking bar model for each of the three levels of feed force. While the overall acceleration magnitudes

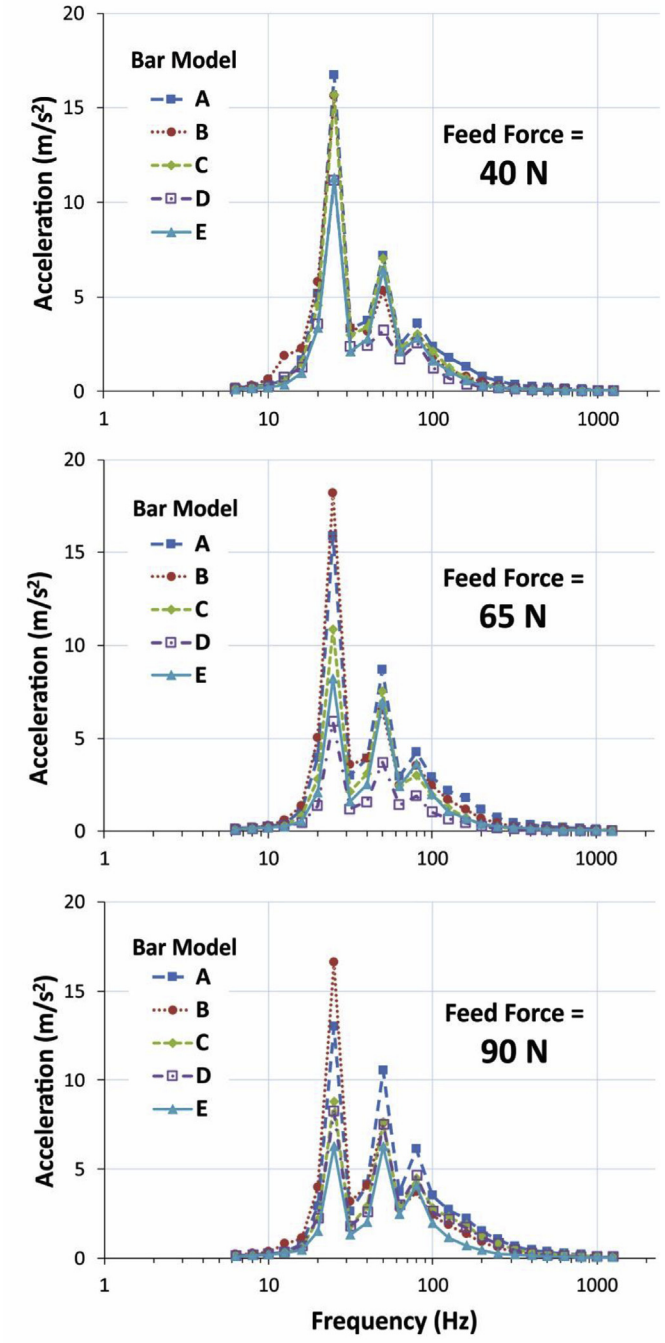


**Fig. 9.** The average one-third octave band vibration frequency spectra measured at the operator's right wrist for the five bucking bar models (A–E) for each of the three feed force levels.

are lower at the wrist than at the bucking bar, Figs. 9 and 11 show some similar trends. As is the case for acceleration measured at the bucking bar, the wrist acceleration means for the spring-damper bars (especially bars C, and D) are more sensitive to the force level effects than are those for the solid metal bars (bars A and B). The spring-damper U.S. Industrial Tool (bar E) exhibited decreased acceleration as the feed force increased at both the bucking bar and the wrist. As was the case for acceleration measured at the bucking bar, the larger of the two Atlas Copco bar models (bar D) exhibited its lowest weighted and unweighted wrist acceleration averages at the middle feed force level (65 N). Different from the trend shown at the bucking bar, Atlas Copco bar C exhibited decreased acceleration at the wrist as feed force increased. Also notably different, while the tungsten alloy bar model (bar B) had significantly lower acceleration at the bucking bar as compared to the steel model (bar A), this was not the case for acceleration measured at the wrist. In fact, the frequency-weighted wrist acceleration mean for bar B (12.3 m/s$^2$) was higher than that for bar A (11.2 m/s$^2$); the unweighted wrist acceleration means for bars A and B were equal (20.6 m/s$^2$).

The ANOVA results for acceleration measured at the wrist were quite similar to those for acceleration measured at the bucking bar. For frequency-weighted wrist acceleration, force level ($F_{2,696} = 66.2$; $p < 0.001$), bar model ($F_{4,696} = 189.8$; $p < 0.001$), and the force level by bar model interaction ($F_{8,696} = 13.1$; $p < 0.001$) were all significant factors. Likewise for unweighted wrist acceleration, force level ($F_{2,696} = 15.6$; $p < 0.001$), bar model ($F_{4,696} = 191.2$; $p < 0.001$), and the force level by bar model interaction ($F_{8,696} = 16.2$; $p < 0.001$) were all significant factors. Post hoc Tukey tests for force level showed that for frequency-weighted acceleration at the wrist, all means were significantly different from one another ($p < 0.05$); the lowest feed force (40 N) produced the highest weighted acceleration followed by the 65 N force and the 90 N feed force. For unweighted wrist acceleration, the means for the 65 N and 90 N trials were not statistically different ($p > 0.05$), but they were both significantly lower than the 40 N mean ($p < 0.05$). In terms of frequency-weighted wrist acceleration, bar B produced the highest acceleration mean followed by bars A, C, E, and D. Tukey test results for bar model for weighted wrist acceleration showed that all bar model means were significantly different except for bars E and D. The rank order for unweighted wrist acceleration from highest acceleration to lowest was A, B, C, E, and D. Tukey test results for bar model for unweighted wrist acceleration showed that bars A and B were not statistically different, but were significantly higher than all the other bar models ($p < 0.05$). The Bar C mean was significantly higher than bars E and D ($p < 0.05$), while there was no statistical difference between bars E and D ($p > 0.05$).

Note: For one of the bucking bar operators, the acceleration data recorder at the wrist was inadvertently switched off during data collection for one of the two samples of bucking bar model C. Therefore, the sample sizes for the wrist acceleration data analyses were slightly different than those for the bucking bar and riveting hammer acceleration analyses. Naturally, this missing data also effects the degrees-of-freedom for the terms in the wrist acceleration ANOVAs.

## 4. Discussion and conclusions

This study investigated the effects of feed force on the vibrations of several typical rivet bucking bars and that transmitted to the bucking bar operator's wrist. This study provides useful information for enhancing the understanding of bucking bar responses to vibration excitation from a riveting hammer. This study also provides relevant information that can be used to help develop a standardized laboratory-based bucking bar evaluation methodology and to help select appropriate bucking bars for various workplace riveting applications.

### 4.1. Consistency of the vibration source

A stable and consistent percussive excitation is a basic condition for valid rivet bucking bar screening evaluations. The results (see Fig. 5) indicate that the bucking bar model, feed force level, or the bucking bar operator have no meaningful effects on the riveting hammer vibration. This is because the riveting hammer is firmly secured to the concrete base of the apparatus, and the hammer does not directly act on the bucking bar; the energy absorber serves as a cushion and filter to reduce the effect of bucking bar-related variations on the vibration source. These findings, along with those of our earlier study (McDowell et al., 2015), suggest that the test apparatus proposed by NIOSH researchers meets the basic requirements for a stable vibration source in laboratory-

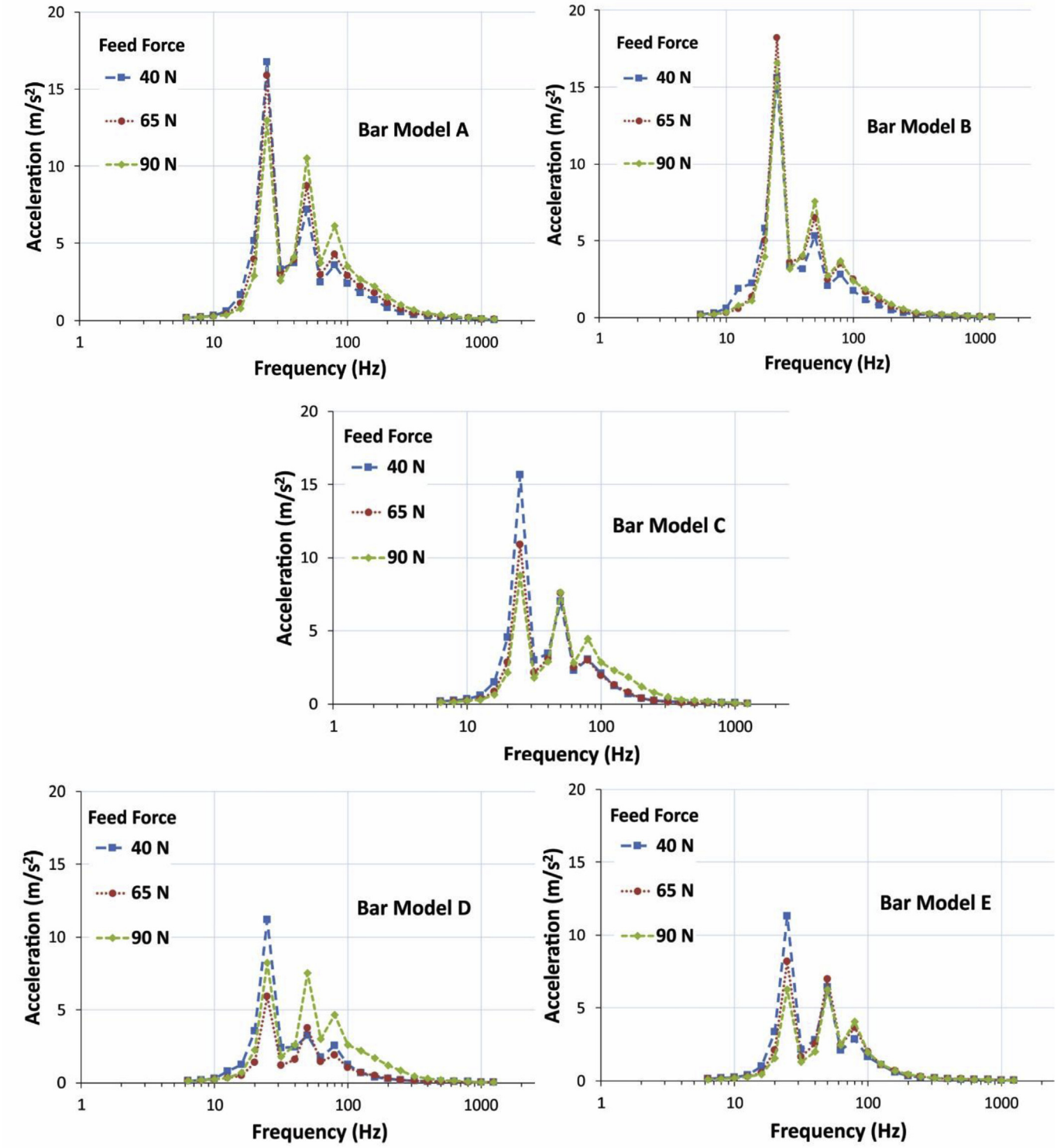


**Fig. 10.** The effect of feed force on the average one-third octave band vibration frequency spectra measured at the operator's right wrist for each bucking bar model.

based bucking bar vibration assessments. This also suggests that the differences among the bucking bar model responses and the feed force effects identified in this study are reliable.

### 4.2. The effect of feed force on bucking bar vibration

The study results shown in Figs. 6–8 demonstrate that the feed force can be a major influencing factor on bucking bar vibrations. A similar feed force effect was observed in an earlier chipping hammer study (Dong et al., 2004). The basic mechanisms of these tool systems are similar. Specifically, increasing the feed force increases not only the bucking bar contact stiffness at its interface with the working piece, but also the effective or apparent mass of the hand-arm system (Dong et al., 2004, 2005). The increased contact stiffness reduces the travel distance of the bucking bar at its fundamental response frequency (related to the operating frequency of the riveting hammer), but it increases the

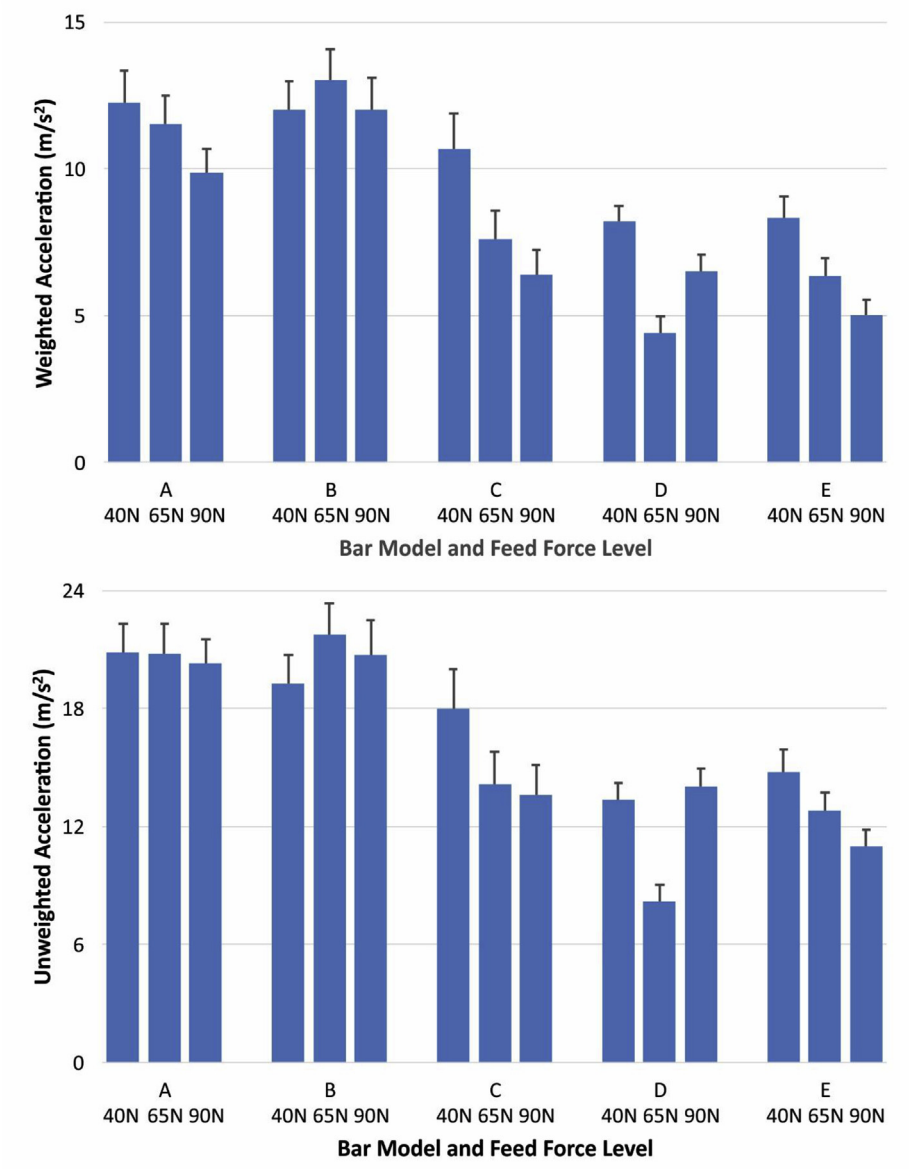


**Fig. 11.** The means for frequency-weighted acceleration (top graph) and unweighted acceleration (bottom graph) measured at the operator's right wrist for each bucking bar model (A–E) and feed force level. Error bars = standard error of the mean (SEM).

intensity of the impact force. While the reduced travel distance reduces the first peak response, the increased sharpness of the impact force increases the high-frequency response. This is the primary reason that as the feed force increases, the magnitude of the first peak generally decreases while the vibration at higher frequencies generally increases, as can be seen in the bucking bar vibration frequency spectra pictured in Figs. 6 and 7. The increased effective mass of the hand-arm system may also have some effect on the bucking bar response, but this effect is frequency-dependent (Dong et al., 2005). While the feed force can substantially increase the hand-arm effective mass at low frequencies, and it may affect the first peak response of the bucking bar, any change of the effective mass at high frequencies should have little effect on the bucking bar vibration because the high-frequency effective mass of the hand-arm system is very small relative to the bucking bar mass (Dong et al., 2004).

Because the first peak has much larger weighting than the remaining peaks (see ISO 5349-1, 2001a), the frequency-weighted acceleration of the bucking bar generally decreases with the increase in the feed force, as shown in Fig. 8. Because the high-frequency vibration generally increases with the increase in the feed force, the unweighted vibration tends to increase at higher feed forces, which can also be observed in Fig. 8. These phenomena are also consistent with those observed in our earlier chipping hammer study (Dong et al., 2004).

As also shown in Fig. 8, bucking bar model D (and to a lesser extent bar model C) is an exception; bar model D exhibited its lowest weighted and unweighted accelerations at the middle feed force level (65 N). This is because bar models C and D are equipped with shock absorbers. These spring-damper systems can effectively isolate the vibration transmission from the bucking member to the bar body held in the operator's hand. However, the spring becomes fully compressed and “bottoms out” with a feed force around 80 N. Beyond that force level, the shock absorber becomes largely ineffective, and the vibration transmitted to the bar body increases. This suggests that to minimize the vibration exposure, this bucking bar should be used for riveting tasks requiring a feed force at about 65 N. Bar model E is also equipped with a spring-damper system, but its spring is much stiffer than those in models C and D. The feed force required to bottom out the spring in bar model E is well above 100 N, so this bar does not have the same feed force limitation.

### 4.3. The effect of feed force on vibration at the bar operator's wrist

As shown in Figs. 9 and 10, the largest acceleration peaks at the wrist occur at 25 and 50 Hz. These two frequency bands are multiples of the operating frequency of the riveting hammer, and are also within the resonant frequency of the hand-wrist-arm system (Dong et al., 2005, 2006). Vibration at frequencies above 250 Hz is largely absorbed by the finger and palm tissues. As a result, such vibration cannot be effectively transmitted to the wrist. This explains why little vibration on the wrist was observed in the high-frequency range, as also shown in Figs. 9 and 10. While the acceleration magnitudes were lower at the wrist than at the bucking bar, some similar trends can be observed in Fig. 8 (bar acceleration) and 11 (wrist acceleration). With the exception of bar model C, the feed force effect on bar acceleration is very similar to the effect observed at the wrist. This is true for both frequency-weighted and unweighted acceleration.

As also shown in Fig. 8, the tungsten alloy bucking bars (bar model B) exhibited reduced bucking bar acceleration levels as compared to their cold-rolled steel twins (bar model A). However, this was not the case for acceleration measured at the wrist (Fig. 11). Depending on the feed force level, bar model B actually produced similar or higher wrist weighted and unweighted acceleration levels than bar model A. This is due to the fact that the heavier tungsten alloy bar effectively attenuates high-frequency vibration, but this bar cannot mitigate lower-frequency components. Therefore, the tungsten bars can offer protection against vibrations transmitted to the bar operator's fingers where the resonant frequency is in the frequency range of 100–300 Hz (Dong et al., 2005, 2007), but this bucking bar design offers little mitigation of vibration exposure to the operator's wrist.

### 4.4. Implications for the standardization of laboratory-based bucking bar assessments

To ensure that the vibration source is stable and consistent, the vibration on the riveting hammer should be measured and reported in laboratory-based bucking bar vibration evaluations. The percussive vibration may vary with the model of riveting hammer and its air pressure supply. A commonly-available and representative model of riveting hammer should be specified in the standardized method. The pressure and volume of the riveting hammer air supply should be consistent with the specifications provided by the riveting hammer manufacturer. These measures, however, may not fully assure the consistency of the vibration directly acting on the bucking bars at different laboratories; different samples of the same model of riveting hammer may generate marginally different vibration spectra, and the mounting configurations and the construction of the energy absorber may vary slightly from lab to lab. The vibration properties of the riveting hammer and energy absorber may also gradually change with use. Such variations can be taken into account by considering a standard calibration bucking bar (with certain dimensions, material, and mass) in the assessment.

The feed forces applied to bucking bars in workplace sheet metal riveting applications varies from task to task depending on the rivet size, rivet composition, sheet metal thickness, and other factors, and feed force is an important factor influencing rivet quality (Cheraghi, 2008). This study shows that different bucking bar designs will respond differently to variations in feed force. This means that the feed force required for a specific riveting operation should be an important consideration when selecting appropriate bucking bar models. To help in the informed selection of bucking bars, candidate bar models should be evaluated at multiple feed force levels. The results of this study suggest that at least three levels of feed force should be considered in bucking bar vibration evaluations. This is especially true for bucking bars featuring spring-damper systems; this study has shown that these models are particularly sensitive to changes in feed force, and these bars are optimized for certain feed force ranges. In all cases, the feed force levels used in bucking bar evaluations should be representative of the feed forces observed in actual workplace riveting applications.

In addition to evaluating the vibration at the bucking bar, the vibration at the wrist should also be measured as additional information for assessing and selecting rivet bucking bars. As observed in this study, some bucking bar designs may offer reduced vibration exposures to the bar operator's fingers while providing little attenuation of wrist acceleration. Knowledge of such trade-offs can be important for making informed rivet bucking bar selections.

## Disclaimer

The findings and conclusions in this report are those of the authors and do not necessarily represent the official position of the National Institute for Occupational Safety & Health, Centers for Disease Control & Prevention. The mention of trade names, commercial products, or organizations does not imply endorsement by the U.S. Government.

## References


Ando, H., Nieminen, K., Toppila, E., Starch, J., Ishitake, T., 2005. Effect of impulse vibration on red blood cells in vitro. Scand. J. Work. Environ. Health 31 (4), 286–290.

ANSI, 2006. ANSI S2.70: Guide for the Measurement and Evaluation of Human Exposure to Vibration Transmitted to the Hand (Revision of ANSI S3.34-1986). American National Standards Institute (ANSI), New York.

Besa, A.J., Valero, F.J., Suner, J.L., Carballeira, J., 2007. Characterisation of the mechanical impedance of the human hand-arm system: the influence of vibration direction, hand-arm posture and muscle tension. Int. J. Ind. Ergon. 37, 225–231.

Burdorf, A., Monster, A., 1991. Exposure to vibration and self-reported health complaints of riveters in the aircraft industry. Ann. Occup. Hyg. 35 (3), 287–298.

Burström, L., Lundström, R., 1994. Absorption of vibration energy in the human hand and arm. Ergonomics 37 (5), 879–890.

Campbell, F.C., 2006. Chapter 11-Structural Assembly Manufacturing Technology for Aerospace Structural Materials. Elsevier Science, Oxford, pp. 495–537.

Cheraghi, S.H., 2008. Effect of variations in the riveting process on the quality of riveted joints. Int. J. Adv. Manuf. Technol. 39, 1144–1155.

Dandanell, R., Engstrom, K., 1986. Vibration from riveting tools in the frequency range 6 Hz-10 MHz and Raynaud's phenomenon. Scand. J. Work. Environ. Health 12, 338–342.

Dong, J.H., Dong, R.G., Rakheja, S., Wu, J.Z., 2007. Predictions of the Distributed Biodynamic Responses in the Hand-arm System Proceedings of the 11th International Conference on Hand-arm Vibration. pp. 359–368 Bologna, Italy.

Dong, R.G., McDowell, T.W., Welcome, D.E., 2005. Biodynamic response at the palm of the human hand subjected to a random vibration. Ind. Health 43 (1), 241–255.

Dong, R.G., McDowell, T.W., Welcome, D.E., Warren, C., Schopper, A.W., 2004. An evaluation of the standardized chipping hammer test specified in ISO 8662-2, 1992. Ann. Occup. Hyg. 48 (1), 39–49.

Dong, R.G., Welcome, D.E., McDowell, T.W., Wu, J.Z., 2006. Measurement of biodynamic response of human hand-arm system. J. Sound Vib. 294 (4–5), 807–827.

Engström, K., Dandanell, R., 1986. Exposure conditions and Raynaud's phenomenon among riveters in the aircraft industry. Scand. J. Work. Environ. Health 12, 293–295.

EU, 2002. Directive 2002/44/EC of the European Parliament and the Council of 25 June 2002 on the Minimum Health and Safety Requirements Regarding the Exposure of Workers to the Risks Arising from Physical Agents (Vibration) (16th Individual Directive within the Meaning of Article 16(1) of Directive 89/391/EEC). The European Parliament and the Council of the European Union (EU), Luxembourg.

Fredericks, T., Fernandez, J., 1999. The effect of vibration on psychophysically derived work frequencies for a riveting task. Int. J. Ind. Ergon. 23, 415–429.

Gemne, G., Saraste, H., 1987. Bone and joint pathology in workers using hand-held vibration tools. Scand. J. Work. Environ. Health 13, 290–300.

Govindaraju, S.R., Rogness, O., Persson, M., Bain, J., Riley, D.A., 2011. Vibration from a riveting hammer causes severe nerve damage in the rat tail model. Muscle Nerve 44, 795–804.

Griffin, M.J., 1990. Handbook of Human Vibration. Academic Press, London.

ISO, 1992. ISO 8662-2: Hand-held Portable Power Tools – Measurement of Vibrations at the Handle – Part 2: Chipping Hammers and Riveting Hammers. International Organization for Standardization, Geneva, Switzerland.

ISO, 1997. ISO 8662-8667: Hand-held Portable Power Tools – Measurement of Vibrations at the Handle – Part 7: Wrenches, Screwdrivers, and Nut Runners with Impact, Impulse, or Ratchet Action. International Organization for Standardization, Geneva, Switzerland.

ISO, 2001a. ISO 5349-1: Mechanical Vibration – Measurement and Evaluation of Human Exposure to Hand-transmitted Vibration – Part 1: General Requirements. International Organization for Standardization, Geneva.

ISO, 2001b. ISO 5349-2: Mechanical Vibration – Measurement and Evaluation of Human Exposure to Hand-transmitted Vibration – Part 2: Practical Guidance for Measurement at the Workplace. International Organization for Standardization, Geneva, Switzerland.

ISO, 2011. ISO 28927-10 – Hand-held Portable Power Tools – Test Methods for Evaluation of Vibration Emission – Part 10: Percussive Drills, Hammers and Breakers.

International Organization for Standardization, Geneva.
Jorgensen, M.J., Viswanathan, M., 2005. Ergonomic field assessment of bucking bars during riveting tasks. In: Proceedings of the Human Factors and Ergonomics Society 49th Annual Meeting - 2005, pp. 1354–1358 Orlando, FL, USA.
Kattel, B., Fernandez, J., 1999. The effects of rivet guns on hand-arm vibration. Int. J. Ind. Ergon. 23, 595–608.
Krajnak, K., Waugh, S., Johnson, C., Miller, G.R., Xu, X.S., Warren, C., Dong, R.G., 2013. The effects of impact vibration on peripheral blood vessels and nerves. Ind. Health 51, 572–580.
Marcotte, P., Aldien, Y., Boileau, P.E., Rakheja, S., Boutin, J., 2005. Effect of handle size and hand-handle contact force on the biodynamic response of the hand-arm system under Zh-Axis vibration. J. Sound Vib. 283, 1071–1091.
McDowell, T.W., Marcotte, P., Warren, C., Welcome, D.E., Dong, R.G., 2009. Comparing three methods for evaluating impact wrench vibration emissions. Ann. Occup. Hyg. 53 (6), 617–626.
McDowell, T.W., Warren, C., Welcome, D.E., Dong, R.G., 2012. Laboratory and field measurements of vibration at the handles of selected riveting hammers. Ann. Occup. Hyg. 56 (8), 911–924.
McDowell, T.W., Warren, C., Xu, X.S., Welcome, D.E., Dong, R.G., 2015. Laboratory and workplace assessments of rivet bucking bar vibration emissions. Ann. Occup. Hyg. 59 (3), 382–397.
McKenna, K.M., McGrann, S., Blann, A.D., Allen, J.A., 1993. An investigation into the acute vascular effects of riveting. Br. J. Ind. Med. 50 (2), 160–166.
NIOSH, 1997. Musculoskeletal Disorders and Workplace Factors: a Critical Review of Epidemiologic Evidence for Work-related Musculoskeletal Disorders of the Neck, Upper Extremity, and Low Back. NIOSH Publication 97–141. U.S. Department of Health and Human Services, National Institute for Occupational Safety and Health, Cincinnati, OH.
SAE, 2014. AS6228-Safety Requirements for Procurement, Maintenance and Use of Hand-held Powered Tools SAE International. (Warrendale, PA, USA).
Treskog, E., 1994. Atlas Copco Tools AB - Technical Report 1994-03-08: Handheld Portable Power Tools. Measurements of Vibrations at the Handle - Bucking Bars. Atlas Copco, Stockholm.
Xi, F.-F., Yu, L., Tu, X.-W., 2013. Framework on robotic percussive riveting for aircraft assembly automation. Adv. Manuf. 1 (2), 112–122.
Yu, Z.S., Chao, H., Qiao, L., Qian, D.S., Ye, Y.H., 1986. Epidemiologic survey of vibration syndrome among riveters, chippers and grinders in the railroad system of the People's republic of China. Scand. J. Work. Environ. Health 12 (4 Special Issue), 289–292.